Phosphorylation of C-terminal polycystin-2 influences the interaction with PIGEA14: A QCM study based on solid supported membranes

Daniela Morick [a], Michaela Schatz [a], Raphael Hubrich [a], Helen Hoffmeister [b], Anya Krefft [b], Ralph Witzgall [b], Claudia Steinem [a,*]

[a] Institut für Organische und Biomolekulare Chemie, Georg-August Universität, Tammannstraße 2, 37077 Göttingen, Germany
[b] Universität Regensburg, Universitätsstraße 31, 93053 Regensburg, Germany

ABSTRACT

Polycystin-2 (PC2) trafficking has been proposed to be a result of the interaction of PIGEA14 with PC2 as a function of the phosphorylation state of PC2. Here, we investigated the interaction of PIGEA14 with the C-terminal part of polycystin-2 wild type (cPC2wt) and the pseudophosphorylated mutant (cPC2S812D) to first, quantify the binding affinity between cPC2 and PIGEA14 and second, to elucidate the influence of PC2 phosphorylation on PIGEA14 binding. Solid supported membranes composed of octanethiol/1,2-diol-eoyl-*sn*-glycero-3-phosphocholine doped with the receptor lipid DOGS–NTA–Ni were used to attach PIGEA14 to the membrane via its hexahistidine tag. By means of the quartz crystal microbalance technique, binding affinities as well as kinetic constants of the interaction were extracted in a label-free manner by applying the scaled particle theory. The results show that the dissociation constant of cPC2 to PIGEA14 is in the 10 nM regime providing strong evidence of a very specific interaction of cPC2 with PIGEA14. The interaction of cPC2wt is twofold larger than that of cPC2S812D. The moderate higher binding affinity of cPC2wt to PIGEA14 is discussed in light of PC2 trafficking to the plasma membrane.

© 2013 Elsevier Inc. All rights reserved.

1. Introduction

The *PKD2* gene is known to be mutated in 15% of all patients with autosomal dominant polycystic kidney disease (ADPKD), which is one of the most common inherited human renal diseases (prevalence of ~1:800) [1,2]. *PKD2* encodes for the transmembrane protein polycystin-2 (PC2) [3–5]. PC2 is a member of the transient receptor potential ion channel family and functions as a Ca^{2+}-permeable cation channel [6,7]. The C-terminus of PC2 (cPC2) harbors one accepted and one proposed coiled-coil domain between Glu^{772}–Leu^{796} and Phe^{839}–Asp^{919}, which facilitate protein–protein interactions, and an EF-hand motif (Ala^{711}–Pro^{797}) as a potential Ca^{2+} binding site [8]. The C-terminal region of PC2 exhibits a retention signal for the endoplasmic reticulum (ER) composed of a cluster of acidic amino acid residues (Asp^{790}–Ser^{820}) and two known phosphorylation sites at Ser^{801} and Ser^{812} [9,10].

The subcellular localization of PC2 still remains a matter of discussion. Depending on the cell line and cellular conditions, PC2 was found at the ER, the plasma membrane and at the primary cilium [11,12]. The subcellular distribution of PC2 strongly influences the possibility of polycystin-1 (PC1)/PC2 complex formation as well

as its function, which plays a crucial role in kidney development. While in primary cilia, the Ca^{2+}-channel activity of PC2 is induced by fluid shear stress and regulates tissue development [13], the PC1/PC2 complex at the plasma membrane is implicated in cell–cell and cell-matrix adhesion [14,15]. Köttgen et al. [16] discovered that the subcellular distribution of PC2 is directed by binding to phosphofurin acidic cluster sorting proteins PACS-1 and PACS-2. It is proposed that PC2 transport is guided by the phosphorylation state of Ser^{812} of PC2, which alters its interaction with PACS-1 and PACS-2 as well as with PIGEA14 (polycystin-2 interactor, Golgi- and endoplasmic reticulum-associated protein with a mass of 14 kDa) (Fig. 1).

PIGEA14 was first identified as a PC2 interacting protein employing a yeast-two-hybrid screen with the C-terminus of PC2 [17]. Co-expression of PC2 and PIGEA14 cDNA in HeLa cells showed a redistribution of these proteins from the ER to the trans-Golgi network. In another two-hybrid screen with PIGEA14 as the bait protein, GM130 was isolated as binding partner, which is a component of the cis-Golgi compartment. It has been shown that the C-terminus of PIGEA14 harbors a coiled-coil domain between residue 73 and 100 [18], which is essential for its interaction with PC2 [17,19]. These results imply that PIGEA14 might facilitate PC2 transport from the ER to the Golgi [20] and it is conceivable that the interaction of PIGEA14 with PC2 is altered by the phosphorylation of PC2 at Ser^{812}.

* Corresponding author. Fax: +49 551 3933228.
  E-mail address: csteine@gwdg.de (C. Steinem).
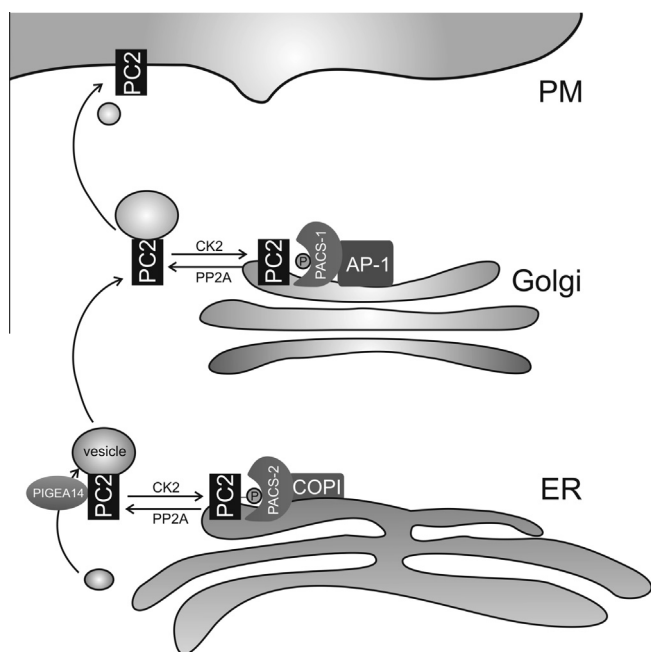
Fig. 1. Postulated mechanism of PC2 trafficking. PC2, phosphorylated by casein kinase 2 (CK2) at Ser[812], is retrieved at the endoplasmic reticulum (ER) via binding to PACS-2/COPI. Desphosphorylation of PC2 by protein phosphatase 2 A (PP2A) facilitates its translocation to the Golgi compartment. This transport is governed by binding to PIGEA14. Retrieval at the Golgi compartment is mediated by PACS-1/adaptin protein-1 (AP-1) to phosphorylated PC2. Dephosphorylation and further unknown factors facilitate PC2 trafficking to the plasma membrane.

To provide evidence for this hypothesis, first we quantitatively investigated the interaction of PC2 with PIGEA14 and second, elucidated the influence of the phosphorylation of PC2 making use of a recently established assay [21] based on the quartz crystal microbalance (QCM) technique [22–24], which allowed us to monitor protein–protein complex formation in a time-resolved and label-free manner. Our results unambiguously demonstrate that the the C-terminal part of PC2 interacts very specifically with PIGEA14 and further suggest that the phosphorylation of cPC2 might alter its binding affinity to PIGEA14, which can be discussed in light of the proposed model of PC2 recruitment tothe plasma membrane (Fig. 1).

2. Materials and methods

2.1. Protein expression and purification

The C-terminal parts (Gly[679]–Val[968]) of polycystin-2 wild type (cPC2wt) and the pseudophosphorylated mutant cPC2S812D were recombinantly expressed in *Escherichia coli* (Rosetta pLys strain) with the expression vector pMAL-c2/TEV-pkd2c. PIGEA14 was expressed in *E. coli* (strain BL21(DE3)) containing the expression vector pET21b/CIP1 (116/493). A detailed description of the procedures is found in the Supplementary information.

2.2. Vesicle preparation

Mixed lipid films composed of 1,2-dioleoyl-*sn*-glycero-3-phosphocholine (DOPC)/Ni^{2+} salt of 1,2-dioleoyl-*sn*-glycero-3-[(N-(5-amino-1carboxypentyl)iminodiacetic acid) succinyl] (DOGS–NTA–Ni), 9:1 (Avanti Polar Lipids, Alabaster, Al, USA) were prepared at the bottom of glass test tubes by removing chloroform under a stream of nitrogen at 32 °C followed by drying at 32 °C for 3 h under vacuum and stored at 4 °C until use. Multilamellar vesicles

(MLVs) were obtained after rehydrating the lipid film in buffer-B (500 mM NaCl, 20 mM Tris/HCl, pH 8.0) for 30 min and periodically vortexing the mixture for 30 s every 5 min. MLVs were converted to small unilamellar vesicles (SUVs) by sonication using a tip-sonifier (3 × 10 min periods, 60% power, 4 cycles, sonifer tip, Bandelin Sonoplus, Berlin, Germany). SUV suspensions were used within 2 h and kept at 4 °C until used.

2.3. Preparation of hybrid SSMs

Chromium (5 nm, Bal-Tec, Balzer, Liechtenstein) and gold (100 nm, Allgemeine Gold- und Silberscheideanstalt AG, Pforzheim, Germany) were evaporated on a 5 MHz AT cut quartz crystal (0.33 mm thickness, 14 mm diameter, 0.25 cm^2 gold electrode area, KVG, Neckarbischofsheim, Germany) at 8·10^{-6} mbar on a MED020 evaporation unit (Bal TEC GmbH, Witten, Germany). Hybrid solid supported membranes (SSMs) composed of octanethiol-DOPC/DOGS–NTA–Ni (9:1) were prepared on the gold electrodes by first cleaning the quartz crystal by argon plasma for 5 min (Plasma Cleaner, Harrick, NY, USA) followed by immersing them in an ethanolic octanethiol solution (10 mM, Sigma–Aldrich, Steinheim, Germany) for 2 h at room temperature. After rinsing with ethanol and buffer-B, the quality of the self-assembled monolayer (SAM) was controlled by impedance spectroscopy (SI 1260, Solartron Instruments, Farnborough, UK). A specific capacitance of (2.3 ± 0.2) μF/cm^2 indicated successful SAM formation. The second monolayer on top of the SAM to form a hybrid SSM was generated by incubating with an SUV suspension (0.2 mg/ml) for 1.5 h at room temperature. The surface was rinsed with buffer-B and the quality of the resulting SSM was confirmed by the capacitance of the bilayer of (1.1 ± 0.2) μF/cm^2.

2.4. CD spectroscopy

Circular dichroism (CD) spectra were recorded using a Jasco-810 spectropolarimeter. Seven averaged CD spectra of cPC2wt and cPC2S812D (4–6 μM) were recorded in 20 mM KH$_2$PO$_4$/K$_2$HPO$_4$, 1 mM EDTA, pH 7.4 at 20 °C using a 1 mm quartz glass cuvette from 270 to 190 nm, at a scan speed of 20 nm/min. Spectra were background corrected, smoothed and evaluated using the on-line server DICHROWEB (CDSSTR algorithm, reference set 7).

2.5. QCM measurements

Quartz crystal microbalance (QCM) experiments were performed using the amplitude controlled QCM200 (Stanford Research Systems, Sunnyvale, CA, USA). A Teflon chamber harboring the AT cut quartz crystal was used as flow through cell with an inlet and outlet connected to a peristaltic pump that allows buffer and protein transport (flow rate: 0.4 mL/min) to one side of the quartz surface with a stagnation flow point geometry. Changes in resonance frequency Δf and changes in the dynamic resistances ΔR were read out in real time with a personal computer connected to the QCM200. All measurements were performed at 20 °C.

2.6. Kinetic modeling of the data

To overcome major drawbacks of the Langmuir model, we applied a model based on the scaled particle theory (SPT) to evaluate the kinetics of protein binding [21]. The model takes into account that proteins might expand over more than one lattice space, which leads to a maximal surface coverage of less than 100%. It further includes mass transport effects as a difference of particle density in bulk solution ρ_∞ and at the sensor surface $\rho(\delta)$. These two refinements lead to:

$$\frac{d\theta}{dt} = \frac{k_{\mathrm{on}}c\Phi(\theta) - k_{\mathrm{off}}\theta}{1 + \frac{k_{\mathrm{on}}}{k_{\mathrm{tr}}}\Phi(\theta)} \qquad (1)$$

with the rate constants of adsorption (k_{on}), desorption (k_{off}) and transport from bulk solution to the sensor surface (k_{tr}), surface coverage (θ), available surface function $\Phi(\theta)$ and concentration of the molecules in bulk solution (c). As a compact analytical expression of $\Phi(\theta)$ cannot be achieved, the SPT approach is used to calculate $\Phi(\theta)$:

$$\Phi(\theta) = (1 - \theta)\exp\left[-3\frac{\theta}{1-\theta} - \left(\frac{\theta}{1-\theta}\right)^2\right], \qquad (2)$$

which provides accurate results up to high surface coverage near the jamming limit. For analysis of the kinetics, a MATLAB routine with a Nelder–Mead algorithm was used as previously described [21].

3. Results

3.1. Expression, purification and characterization of PIGEA14

To obtain high yields of soluble active PIGEA 14 and to minimize the formation of inclusion bodies, protein expression was performed at $T = 30\,^{\circ}\mathrm{C}$ rather than at 37 °C [25,26]. Functional protein was only obtained by purification with a Ni–iminodiacetic acid (Ni–IDA) agarose column using 50 mM EDTA. If a commonly applied Ni–nitrilotriacetic acid (Ni–NTA) agarose was used, purification of the PIGEA14 cell lysate turned out to be unsuccessful. The use of imidazole resulted in protein denaturation/precipitation, which was confirmed by means of QCM experiments performed after dialysis in buffer-B. No binding of the hexahistidine tagged protein to a DOGS–NTA–Ni containing membrane was monitored. IDA chelates Ni^{2+} with lower affinity than NTA does and thus PIGEA14 together with Ni^{2+} can be eluted more efficiently with EDTA containing buffer [27]. Protein purity was documented by SDS–PAGE showing PIGEA14 at about 17 kDa (Fig. 1S, Supplementary information). Western blot analysis using a pentahistidine antibody that recognizes the hexahistidine tag (anti His$_5$, Qiagen, Hilden, Germany) confirmed the presence of an accessible histidine tag of PIGEA14 (Fig. 1S, Supplementary information).

3.2. CD analysis of cPC2wt and cPC2S812D

Even though replacing a Ser, or Thr residue by a Glu or Asp residue is a common method to introduce pseudophosphorylations in proteins, a single point mutation can considerably influence the protein structure [28] and can in principle interfere with the protein's ability to specifically bind its interaction partner. To rule out that a change in secondary structure as a result of the S/D exchange is responsible for an altered binding affinity of cPC2, we analyzed the protein structures of cPC2wt and cPC2S812D by CD-spectroscopy. CD spectra of cPC2wt and cPC2S812D (Fig. 2) demonstrated that no significant difference between the two proteins' secondary structures can be deduced. In both cases, 36% α-helix, 13% β-strand, 16% turns and 35% random coil was determined. The calculated α-helicity is in good agreement with the α-helical content of 34% determined by Celić et al. [9] and 30% determined by Schumann et al. [29] for cPC2wt using CD spectroscopy in Ca^{2+} free buffer.

3.3. Immobilization of PIGEA14 on SSMs and interaction with cPC2

To be able to investigate the interaction of PIGEA14 with cPC2wt and cPC2S812D, respectively, PIGEA14 was first bound to a hybrid SSM containing DOGS–NTA–Ni via its histidine tag [21].
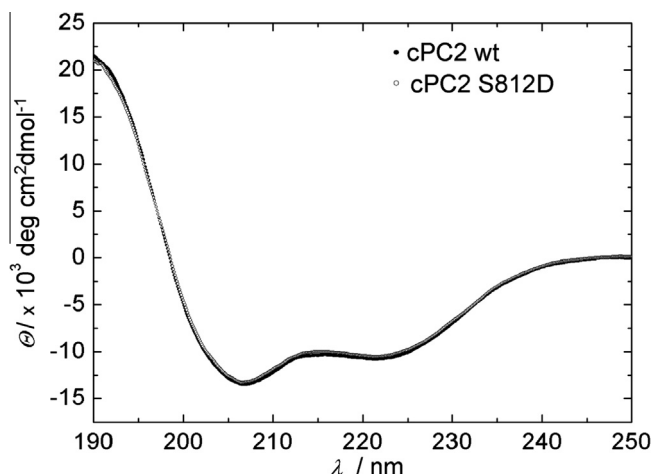
Fig. 2. CD spectra of cPC2wt and cPC2S812D mutant.

Hybrid SSMs composed of DOPC doped with 10 mol% of DOGS–NTA–Ni were used to ensure an almost irreversible immobilization of the hexahistidine-tagged PIGEA14 and maximal surface coverage. In contrast to a covalent attachment of PIGEA14 to the surface, binding of the protein to a SSM allows for lateral mobility of the lipids, which might influence the interaction with cPC2 as a result of conceivable protein reorganization. The lateral mobility of the lipids was verified using fluorescence recovery after photobleaching experiments (Supplementary information). To investigate the specificity of PIGEA14 binding to DOGS–NTA–Ni, control experiments with neat DOPC membranes were performed. The addition of 0.3 μM PIGEA14 did not result in any non-specific binding, i.e. no shift in resonance frequency of the quartz crystal was observed (Fig. 3A). However, the addition of 0.65 μM PIGEA14 to a DOPC/DOGS–NTA–Ni (9:1) hybrid membrane resulted in a significant decrease in resonance frequency of the 5 MHz quartz plate. The change in resonance frequency (Δf) was monitored until the resonance frequency did not further change upon protein addition indicating maximum protein binding. Rinsing with buffer only led to a small increase in resonance frequency, indicating an almost irreversible binding of PIGEA14 (Fig. 3B). A PIGEA14 concentration of 0.8 μM resulted in an average shift in resonance frequency of $-\Delta f_e = (69 \pm 19)$ Hz ($n = 16$), whereas the increase in resonance frequency after rinsing with buffer was below 10% in all cases ($\Delta f_e = (5 \pm 3)$ Hz, $n = 16$).

Prior to the investigation of the cPC2 interaction with PIGEA14, control experiments were performed to rule out any non-specific binding of cPC2 to a protein-covered DOPC/DOGS–NTA–Ni membrane. The hexahistidine-tagged protein ezrin, a protein, which does not specifically interact with cPC2, was bound to the hybrid bilayer composed of DOPC/DOGS–NTA–Ni (9:1). cPC2wt was added up to a concentration of 0.4 μM with no significant change in resonance frequency. This result demonstrates that non-specific binding of cPC2 to a protein-covered membrane can be excluded.

The interaction of PIGEA14 with cPC2wt was then monitored by QCM measurements. cPC2wt was added to a PIGEA14-covered membrane resulting in a characteristic time-dependent decrease in resonance frequency (Fig. 3C) evidencing a specific interaction of cPC2wt with PIGEA14. After reaching a constant frequency value, the shift in resonance frequency at equilibrium was read out to be $\Delta f_e = -14.5$ Hz. As the dynamic resistance ΔR did not change during the binding event, it can be assumed that viscoelastic contributions are negligible. Subsequently after a constant frequency was reached, the system was rinsed with buffer, which led to an increase in resonance frequency of $\Delta f_e = 14.0$ Hz indicating that cPC2wt binding to PIGEA14 is fully reversible. For all QCM experiments, the binding process turned out to be almost fully reversible.
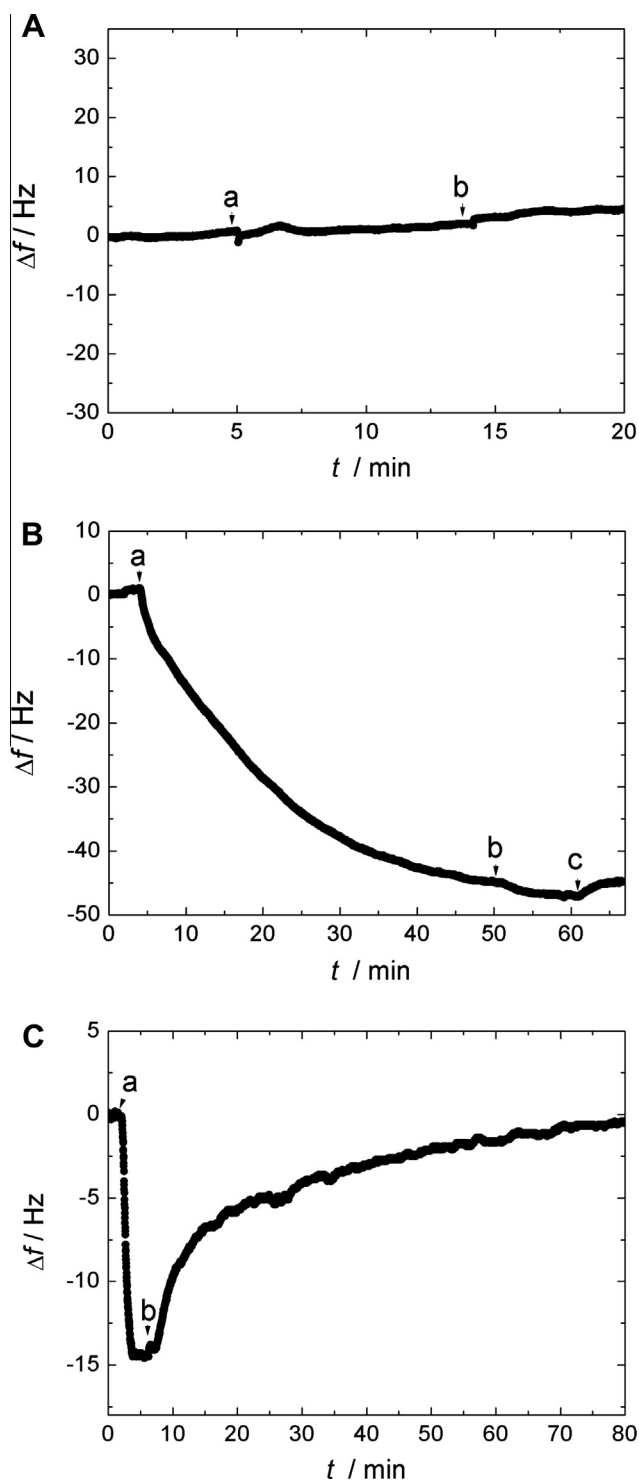
Fig. 3. Time courses of the frequency shifts after addition of: (A) (a) 0.3 µM PIGEA14 to a DOPC–SSM and (b) rinse with buffer-B. (B) (a) 0.65 µM and (b) 0.73 µM PIGEA14 to a DOPC/DOGS–NTA–Ni (9:1)–SSM; (c) indicates the time point of rinsing with buffer-B. (C) (a) 0.27 µM cPC2wt to a DOPC/DOGS–NTA–Ni (9:1)–SSM with bound PIGEA14; (b) indicates the time point of buffer rinsing (150 mM NaCl, 20 mM KH$_2$PO$_4$/K$_2$HPO$_4$, 1 mM EDTA, pH 7.4).

3.4. Binding affinity and kinetics of cPC2wt and cPC2S812D

To quantify the interaction of PIGEA14 with cPC2wt as well as with the cPC2S812D mutant, the change in resonance frequency at equilibrium Δf_e was determined as a function of cPC2 concentration in solution. The obtained Δf_e values were plotted vs. the cPC2

concentration and the parameters of the adsorption isotherm based on the SPT were fit to the data:

$$c_{cPC2} = \frac{K_D \theta}{1-\theta} exp\left[-3\frac{\theta}{1-\theta} - \left(\frac{\theta}{1-\theta}\right)^2\right] \tag{3}$$

with $\theta = \frac{\Delta f_e}{\Delta f_{max}}$. A dissociation constant of $K_D = (64 \pm 22)$ nM was determined for the PIGEA14/cPC2wt interaction (Fig. 4A). The affinity of the pseudophosphorylated mutant cPC2S812D to PIGEA14 was however, two times lower with a dissociation constant of $K_D = (137 \pm 41)$ nM (Fig. 4B).

In addition to the binding affinities, we also analyzed the binding kinetics. Using the known value of K_D, we determined the rate constant of the cPC2 adsorption k_{on} and desorption k_{off}. k_{on} was obtained by a fitting routine of $\Delta f(t)$ based on the SPT (Eq. (2)); k_{off} was calculated from the known dissociation constant according to:

$$K_D = \frac{k_{off}}{k_{on}}. \tag{4}$$

Good agreement between fit and measurements were found (Fig. S2, Supplementary information). The adsorption rate constant k_{on}, desorption rate constant k_{off} along with the rate constant of mass transport k_{tr} are summarized in Table 1.
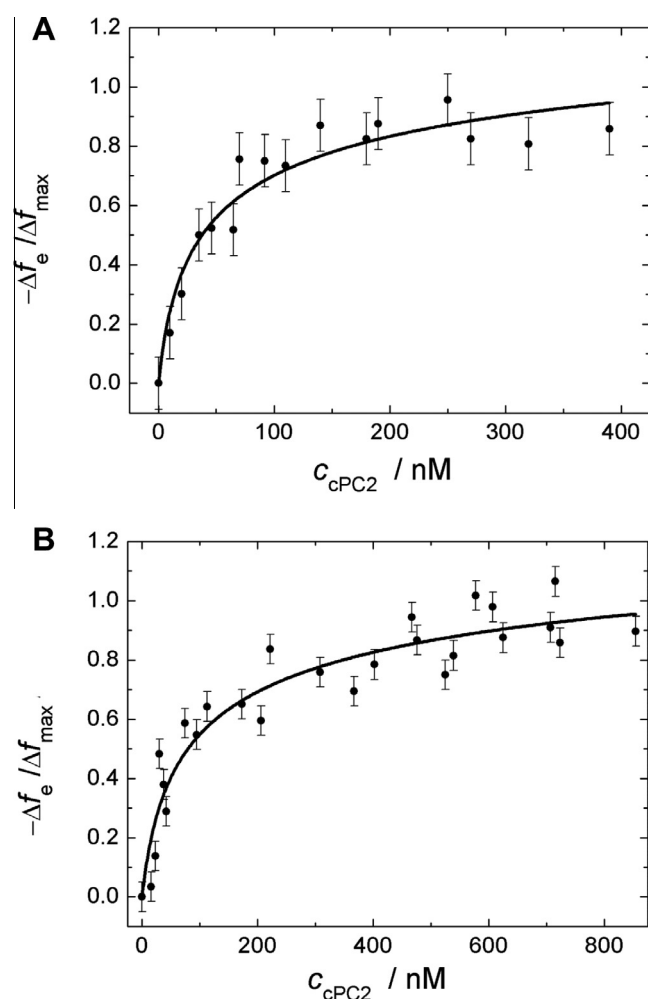
Fig. 4. Adsorption isotherms of (A) cPC2wt ($\Delta f_{max} = (18 \pm 1)$ Hz) and (B) cPC2S812D ($\Delta f_{max} = (23 \pm 1)$ Hz) interacting with PIGEA14. The parameters of Eq. (3) were fit to the data.

Table 1
Summary of the kinetics and thermodynamic parameters of the PIGEA14 interaction with cPC2wt and cPC2S812D.

PIGEA14+	k_{on} ($\times 10^4\,s^{-1}\,M^{-1}$)	k_{off} ($\times 10^{-3}\,s^{-1}$)	k_{tr} ($\times 10^4\,s^{-1}\,M^{-1}$)	K_D (nM)
cPC2wt	10 ± 3	6.7 ± 2.1	4.1 ± 3.6	64 ± 22
cPC2S812D	6.9 ± 2.4	10.9 ± 4.2	1.6 ± 0.6	137 ± 41

4. Discussion

PIGEA14 is the first protein known to date that facilitates forward trafficking of PC2 from the ER to the Golgi compartment [17], which might be influenced by the phosphorylation state of PC2. By means of QCM in conjunction with planar SSMs, we were able to quantify the interaction of the C-terminal domain of PC2 (cPC2) with PIGEA14 bound to a lipid membrane and to elucidate the influence of cPC2 phosphorylation at Ser[812] on this interaction. By using SSMs, the protein–protein interaction is limited to a planar two-dimensional geometry similar to the situation found at cellular membranes. The two dimensional interaction site influences the binding behavior of the proteins, as one interaction partner is localized on a surface, which reduces its translational and rotational degrees of freedom leading to altered binding affinities [30]. A high binding affinity was found for the PIGEA14–cPC2wt interaction providing strong evidence that this interaction is significant also in the cellular environment and might compete with the PACS-PC2 interaction (see Fig. 1). Moreover, we found that the binding affinity of the PIGEA14–cPC2wt interaction is two times larger than that of PIGEA14-pseudophosphorylated cPC2 (cPC2S812D) (Table 1).

The rate constants of association and dissociation of the PIGEA14–cPC2 interaction are in the range of 10^4–$10^5\,M^{-1}\,s^{-1}$ and $10^{-3}\,s^{-1}$, respectively and are also only slightly altered (Table 1) by the pseudophosphorylation of cPC2, as expected. The obtained values are similar to those found for the PC1/cPC2 interaction and are characteristic for biomolecular interactions determined at surfaces [31–33]. For example, Myszka et al. [34] reported association rate constants in the range of 10^3–$10^7\,M^{-1}\,s^{-1}$ for macromolecular interactions obtained with the Biacore® technique. In general, Brownian motion would result in much larger association rate constants in the range of 10^9–$10^{10}\,M^{-1}\,s^{-1}$, which are, however rarely found as the association rate constants are orders of magnitudes smaller as a result of the activation energy of protein complex formation. Dissociation rate constants vary within a wide range of 10^{-6}–$10^{-1}\,s^{-1}$ [35].

Taken together, our results can be discussed in light of the proposed mechanism of PC2 transport (Fig. 1), first proposed by Köttgen et al. [16] and supported by others [36]. The model implies that phosphorylated PC2 binds with high affinity to PACS-2 and thus, remains located at the ER. After dephosphorylation of PC2 at position Ser[812] by protein phosphatase 2A (PP2A), PC2 is released by PACS-2 as the binding affinity is decreased, while the binding affinity of PC2 to PIGEA14 is high and even increased compared to the phosphorylated state as demonstrated by our results. Moreover, the sites of PC2 interacting with PIGEA14 and PACS-2 appear to be in close proximity. Hidaka et al. [17] found that the amino acid sequence Gly[833]–Ser[923] of cPC2 is sufficient to interact with PIGEA14 and this proposed coiled-coil region is in close proximity to the domain responsible for the PC2/PACS interaction [9]. It is conceivable that the high affinity of PC2 to PIGEA14 and the simultaneous change in binding affinity of PC2 to the two different proteins as a result of PC2-phosphorylation might induce the transport of the protein complex to the Golgi network, even though we are aware of the fact that the observed change in affinity is moderate and can only partly explain the situation in vivo.

References

[1] P.C. Harris, V.E. Torres, Polycystic kidney disease, Annu. Rev. Med. 60 (2009) 321–337.
[2] M. Koptides, C.C. Deltas, Autosomal dominant polycystic kidney disease: molecular genetics and molecular pathogenesis, Hum. Genet. 107 (2000) 115–126.
[3] Y. Cai, Y. Maeda, A. Cedzich, V.E. Torres, G. Wu, T. Hayashi, T. Mochizuki, J.H. Park, R. Witzgall, S. Somlo, Identification and characterization of polycystin-2, the *PKD2* gene product, J. Biol. Chem. (1999) 28557–28565.
[4] A. Giamarchi, F. Padilla, B. Coste, M. Raoux, M. Crest, E. Honoré, P. Delmas, The versatile nature of the calcium-permeable cation channel TRPP2, EMBO Rep. 7 (2006) 787–793.
[5] T. Mochizuki, G. Wu, T. Hayashi, S.L. Xenophontos, B. Veldhuisen, J.J. Saris, D.M. Reynolds, Y. Cai, P.A. Gabow, A. Pierides, W.J. Kimberling, M.H. Breuning, C.C. Deltas, D.J. Peters, S. Somlo, *PKD2*, a gene for polycystic kidney disease that encodes an integral membrane protein, Science 272 (1996) 1339–1342.
[6] Y.-J. Hsu, J.G.J. Hoenderop, R.J.M. Bindels, TRP channels in kidney disease, Biochim. Biophys. Acta 1772 (2007) 928–936.
[7] C. Stayner, J. Zhou, Polycystin channels and kidney disease, Trends Pharmacol. Sci. 22 (2001) 543–546.
[8] E.T. Petri, A. Celić, S.D. Kennedy, B.E. Ehrlich, T.J. Boggon, M.E. Hodsdon, Structure of the EF-hand domain of polycystin-2 suggests a mechanism for Ca²⁺-dependent regulation of polycystin-2 channel activity, Proc. Natl. Acad. Sci. USA 107 (2010) 9176–9181.
[9] A. Celić, E.T. Petri, B. Demeler, B.E. Ehrlich, T.J. Boggon, Domain mapping of the polycystin-2 C-terminal tail using de novo molecular modeling and biophysical analysis, J. Biol. Chem. 283 (2008) 28305–28312.
[10] A.J. Streets, A.J. Needham, S.K. Gill, A.C.M. Ong, Protein kinase D-mediated phosphorylation of polycystin-2 (TRPP2) is essential for its effects on cell growth and calcium channel activity, Mol. Biol. Cell 21 (2010) 3853–3865.
[11] M. Köttgen, G. Walz, Subcellular localization and trafficking of polycystins, Pflügers Arch. – Eur. J. Physiol. 451 (2005) 286–293.
[12] R. Witzgall, Polycystin-2-an intracellular or plasma membrane channel?, Naunyn-Schmiedeberg's Arch Pharmacol. 371 (2005) 342–347.
[13] S.M. Nauli, F.J. Alenghat, Y. Luo, E. Williams, P. Vassilev, X. Li, A.E.H. Elia, W. Lu, E.M. Brown, S.J. Quinn, D.E. Ingber, J. Zhou, Polycystins 1 and 2 mediate mechanosensation in the primary cilium of kidney cells, Nat. Genet. (2003) 129–137.
[14] L.J. Newby, A.J. Streets, Y. Zhao, P.C. Harris, C.J. Ward, A.C.M. Ong, Identification, characterization, and localization of a novel kidney polycystin-1-polycystin-2 complex, J. Biol. Chem. 277 (2002) 20763–20773.
[15] L. Tsiokas, Function and regulation of TRPP2 at the plasma membrane, Am. J. Physiol. Renal Physiol. 297 (2009) F1–F9.
[16] M. Köttgen, T. Benzing, T. Simmen, R. Tauber, B. Buchholz, S. Feliciangeli, T.B. Huber, B. Schermer, A. Kramer-Zucker, K. Höpker, K.C. Simmen, C.C. Tschucke, R. Sandford, E. Kim, G. Thomas, G. Walz, Trafficking of TRPP2 by PACS proteins represents a novel mechanism of ion channel regulation, EMBO J. 24 (2005) 705–716.
[17] S. Hidaka, V. Könecke, L. Osten, R. Witzgall, PIGEA-14, a novel coiled-coil protein affecting the intracellular distribution of polycystin-2, J. Biol. Chem. 279 (2004) 35009–35016.
[18] S. Mokhtarzada, C. Yu, A. Brickenden, W.-Y. Choy, Structural characterization of partially disordered human Chibby: insights into its function in the Wnt-signaling pathway, Biochemistry 50 (2011) 715–726.
[19] A. Mofunanya, F.-Q. Li, J.-C. Hsieh, K.-I. Takemaru, Chibby forms a homodimer through a heptad repeat of leucine residues in its C-terminal coiled-coil motif, BMC Mol. Biol. 10 (2009) 41.
[20] R. Witzgall, New developments in the field of cystic kidney diseases, Curr. Mol. Med. 5 (2005) 455–465.
[21] D. Behn, S. Bosk, H. Hoffmeister, A. Janshoff, R. Witzgall, C. Steinem, Quantifying the interaction of the C-terminal regions of polycystin-2 and polycystin-1 attached to a lipid bilayer by means of QCM, Biophys. Chem. 150 (2010) 47–53.
[22] M.A. Cooper, V.T. Singleton, A survey of the 2001 to 2005 quartz crystal microbalance biosensor literature: applications of acoustic physics to the analysis of biomolecular interactions, J. Mol. Recognit. 20 (2007) (2001) 154–184.

[23] A. Janshoff, H.-J. Galla, C. Steinem, Piezoelectric mass-sensing devices as biosensors-an alternative to optical biosensors?, Angew Chem., Int. Ed. 39 (2000) 4004–4032.

[24] J. Wegener, A. Janshoff, C. Steinem, The quartz crystal microbalance as a novel means to study cell–substrate interactions in situ, Cell Biochem. Biophys. 34 (2001) 121–151.

[25] R. Rudolph, H. Lilie, In vitro folding of inclusion body proteins, FASEB J. 10 (1996) 49–56.

[26] C.H. Schein, M.H.M. Noteborn, Formation of soluble recombinant proteins in *Escherichia coli* is favored by lower growth temperature, Nat. Biotechnol. 6 (1988) 291–294.

[27] E. Hochuli, H. Döbeli, A. Schacher, New metal chelate adsorbent selective for proteins and peptides containing neighbouring histidine residues, J. Chromatogr. 411 (1987) 177–184.

[28] S. Bosk, J.A. Braunger, V. Gerke, C. Steinem, Activation of F-actin binding capacity of ezrin: synergism of PIP$_2$ interaction and phosphorylation, Biophys. J. 100 (2011) 1708–1717.

[29] F. Schumann, H. Hoffmeister, R. Bader, M. Schmidt, R. Witzgall, H.R. Kalbitzer, Ca^{2+}-dependent conformational changes in a C-terminal cytosolic domain of polycystin-2, J. Biol. Chem. 284 (2009) 24372–24383.

[30] N. Ben-Tal, B. Honig, C.K. Bagdassarian, A. Ben-Shaul, Association entropy in adsorption processes, Biophys. J. 79 (2000) 1180–1187.

[31] Y.S.N. Day, C.L. Baird, R.L. Rich, D.G. Myszka, Direct comparison of binding equilibrium, thermodynamic, and rate constants determined by surface- and solution-based biophysical methods, Protein Sci. 11 (2002) 1017–1025.

[32] P.-O. Markgren, M.T. Lindgren, K. Gertow, R. Karlsson, M. Hämäläinen, U.H. Danielson, Determination of interaction kinetic constants for HIV-1 protease inhibitors using optical biosensor technology, Anal. Biochem. 291 (2001) 207–218.

[33] M.P. Schwartz, S.D. Alvarez, M.J. Sailor, Porous SiO$_2$ interferometric biosensor for quantitative determination of protein interactions: binding of protein A to immunoglobulins derived from different species, Anal. Chem. 79 (2007) 327–334.

[34] D.G. Myszka, T.A. Morton, M.L. Doyle, I.M. Chaiken, Kinetic analysis of a protein antigen–antibody interaction limited by mass transport on an optical biosensor, Biophys. Chem. 64 (1997) 127–137.

[35] G. Schreiber, Kinetic studies of protein–protein interactions, Curr. Opin. Struct. Biol. 12 (2002) 41–47.

[36] X. Fu, Y. Wang, N. Schetle, H. Gao, M. Pütz, G. Gersdorff, G. Walz, A.G. Kramer-Zucker, The subcellular localization of TRPP2 modulates its function, J. Am. Soc. Nephrol. 19 (2008) 1342–1351.